Medical Image Super-Resolution Reconstruction Algorithms on Deep Learning

Jinglin Yuan

School of Applied Sciences, Macao Polytechnic University, Macau, China
P2316169@mpu.edu.mo

Abstract. The human body's structural details can be more clearly seen in high-resolution MRI and CT pictures, which can also aid in the early identification of disorders. However, due to the limits of imaging technologies, imaging surroundings, and human variables, clean high-resolution photographs are challenging to obtain. For super-resolution reconstruction of medical pictures, I propose a non-subsampled shearlet transform (NSST) and multi-scale information distillation (MSID) network in the current study namely NSST-MSID network. In order to thoroughly investigate the multiscale aspects of images and successfully restore low-resolution photos to high-resolution images, an MSID network that primarily comprises of several cascaded MSID blocks is first proposed. In addition, the super-resolution problem of medical images is characterized as a prediction problem of NSST coefficients, so that the MSID network maintains richer structural details than the spatial domain. This is because existing methods frequently predict high-resolution images in the spatial domain, making the output too smooth and texture details lost. The performance of the suggested strategy is then assessed using the well-known medical image dataset. In comparison to other outstanding methods currently in use, the experimental results demonstrate that the NSST-MSID network can achieve better peak signal-to-noise ratio (PSNR), structural similarity (SSIM), and root-mean-square error (RMSE) values while better preserving local texture details and global topology.

Keywords: Medical image; Super-resolution reconstruction; Convolutional neural networks; MSID; NSST

1 Introduction

Both magnetic resonance imaging (MRI) and computed tomography (CT) make non-invasive medical treatment easier and are particularly useful to doctors when making diagnoses. Medical imaging with high resolution (HR) can give better information about lesions and increase diagnostic precision. However, a variety of issues make the process of acquiring HR medical photos challenging. Medical images are particularly subject to physical restrictions and acquisition time constraints in addition to potential technological limitations. For instance, movement brought on by organ pulsations and patient tiredness can further

B. H. Ahmad (ed.), *Proceedings of the 2023 International Conference on Data Science, Advanced Algorithm and Intelligent Computing (DAI 2023)*, Advances in Intelligent Systems Research 180,
https://doi.org/10.2991/978-94-6463-370-2_41

deteriorate image quality and cause images with worse signal-to-noise ratios (SNR). Super resolution (SR) imaging techniques are therefore becoming increasingly crucial [1-3].

Deep learning (DL) techniques have recently outperformed traditional machine learning algorithms in tasks like image classification [4] and target detection [5], which is largely due to the increase in computational power and the availability of large data. Convolutional neural network (CNN)-based models have greatly raised the quality of SR techniques for SR tasks [6-9]. The shallow structure of the first SRCNN[6] hindered its performance. As a result, researchers have proposed networks with deeper hierarchical structures as VDSR [7], DRRN [8] and Memnet [9] in order to improve performance. Recently, a deeper RCAN model has been proposed [10], which gave extremely satisfactory results in the SR problem. To further enhance the performance, some scholars have proposed super-resolution models incorporating dense connections like SRDenseNet [11] and Memnet [9]. Additionally, more efficient SR approaches based on CNNs connect a collection of similar feature extraction blocks to build the entire network, as shown by RDN [12], IDN [13], MSRN [14], and SRFBN [15], demonstrating the critical importance of each block's performance.

On representative computer vision tasks (target recognition, picture classification, and semantic segmentation), multiscale networks provide good results [14, 16, 17]. Zhang et al. suggested an image SR technique for the SR task that uses multiscale residual networks to adaptively find picture features at various scales [14]. A deep multiscale network for medical image SR was proposed by Wang et al. and can more accurately reflect the overall topology and local texture features of HR medical images [17]. The aforementioned techniques successfully perform image SR in the spatial domain of the image, but they typically result in outputs that are overly smooth and lack texture information. The context and texture information of the image can be preserved at various levels with image SR in the transform domain, which leads in improved SR outcomes. To get HR images by forecasting the "missing details" of wavelet coefficients in low resolution (LR) images, Guo et al. created a deep wavelet super-resolution DWSR network [18]. In addition, Huang et al.’s wavelet transform (WT) application to face SR using convolutional neural network demonstrated that the method can successfully record the local texture information and overall topology data of the face [19].

In the current study, I propose an NSST-MSID network---a non-subsampled shearlet transform and multi-scale information distillation network---for the SR approach for medical images. The MSID network primarily consists of a series of cascaded multi-scale information distillation blocks, which successfully convert LR photos into HR images and thoroughly extract the multi-scale features of medical images. Furthermore, NSST outperforms WT in terms of multiscale, multidirectional, and translation invariant properties. The proposed network contains NSST, validates NSST's superiority over WT, and characterizes the SR problem of medical images as a problem of NSST coefficient prediction, causing the MSID network to further maintain deeper structural information than the

spatial domain.

2 Model Construction

2.1 Overview

In the current study, a medical image SR approach has been proposed concerning the NSST domain MSID network. The method firstly proposes the MSID network, which integrates the multi-scale with the information distillation structure to form a cascaded multi-scale information distillation network, which extracts richer features of long-short paths and facilitates the reconstruction of higher-quality HR medical images. In addition, the implementation of the SR method in the transform domain leads to better texture details and smoother edges in the processed images. Therefore, this paper proposes the use of NSST with superior performance for HR image prediction. Compared with wavelet and curvilinear transforms, NSST has better multi-scale, multi-direction and translation invariant properties, which can better explore the texture and edge features, and further enable the MSID network to retain richer structural details. Specifically, in this paper, a series of cascaded depth MSID blocks are designed in the NSST domain to utilize the rich potential features in medical images for HR image reconstruction. First, a low-frequency component and several high-frequency components are extracted from LR medical images using NSST. The low-frequency component retains global topological information, and the high-frequency component captures structural and textural information. The MSID network is then used to estimate the transform coefficients of the generated HR image using the combination of these components. All the components share a common set of parameters, and these low/high-frequency components are used as inputs to the network to improve the recognition capability more than the null-domain image. Ultimately, these transform coefficients are inverted by NSST to obtain super-resolution reconstructed HR images. The proposed MSID blocks and the prediction of NSST coefficients in the NSST-MSID network are introduced in this part after a description of the proposed MSID network's topology (see Figure 1).

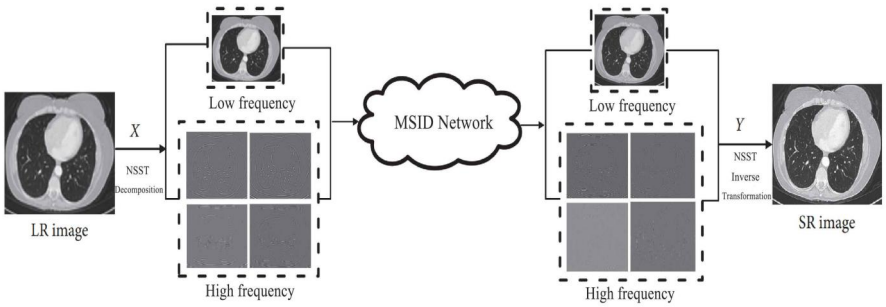

Fig. 1. NSST-MSID network structure (Photo/Picture credit: Original)

2.2 MSID Network Structure

This work proposes an MSID network, compared with traditional multiscale CNNs or multiscale residual networks, the MSID network incorporates cascaded information distillation blocks, extracts the features of local long and short paths, collects as much information as possible using fewer convolutional layers, gradually enriches the effective features for HR image reconstruction, and obtains competitive results. The shallow feature extraction (SFE) module and deep feature extraction (DFE) module make up the two components of the MSID network (see Figure 2). I^{LR} and I^{HR} are used to represent, respectively, LR images and HR pictures. The end-to-end mapping function F between I^{LR} and I^{HR} must be learned as the last step.

$$\theta = \arg\min_{\theta} \frac{1}{N} \sum_{i=1}^{N} L^{SR}\left(F_{\theta}\left(I_i^{LR}\right), I_i^{HR}\right) \tag{1}$$

$\theta = \{w^1, w^2, ..., w^p, b^1, b^2, ..., b^p\}$ denotes the weights and bias parameters of the p convolutional layers; N is the number of training samples; L^{SR} is the loss function minimizing the difference between I^{LR} and I^{HR}.

In image SR techniques, the mean square error function is the most widely employed objective optimization function [8, 9]. The usage of mean square error loss, as demonstrated by Lim et al., has drawbacks, hence in this study, the mean absolute error is used as the loss function instead [20]:

$$L^{SR}\left(F_{\theta}\left(I_i^{LR}\right), I_i^{HR}\right) = \frac{1}{N} \sum_{i=1}^{N} \left\| F_{\theta}\left(I_i^{LR}\right) - I_i^{HR} \right\|_1 \tag{2}$$

To specifically extract shallow features from medical photos, two convolutional layers are used:

$$M_0 = H_{SFE1}\left(H_{SFE2}(I^{LR})\right) \tag{3}$$

Where H_{SFE1} and H_{SFE2} stand for the two SFE module layers' respective convolution processes. Following the shallow feature module, the DFE module, which comprises a series of cascaded MSID blocks, uses the shallow features. Each MSID block can gather as much data as feasible and then extrapolate more insightful data. A 1 * 1 convolutional layer is subsequently used to feature-fuse the output data:

$$M_{GF} = H_{GFE}([M_1, M_2, ..., M_T]) \tag{4}$$

Where $[M_1, M_2, ..., M_T]$ signifies the cascade of feature maps produced by MSID blocks 1, 2, ..., T, H_{GFE} is the fusion function of 1 * 1 convolutional layers. After the features are fused, the feature map I_{Output} is obtained by global residual learning:

$$I_{Output} = M_{GF} + M_0 \tag{5}$$

Except for the feature fusion layer, which has 128 filters, all convolutional layers in the MSID network are constructed with 64 filters.

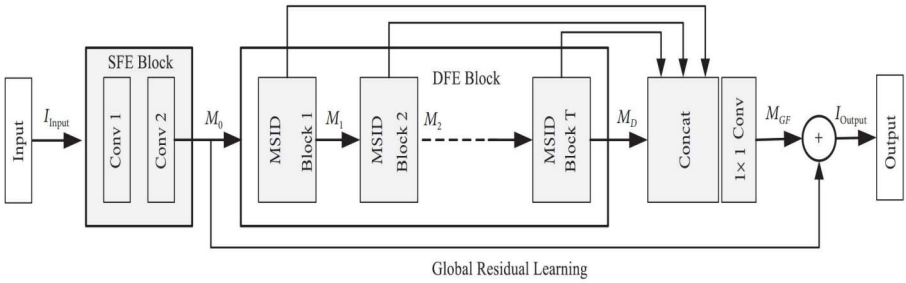

Fig. 2. MSID network workflow (Photo/Picture credit: Original)

2.3 MSID block

There are two sections to each MSID block that can be utilized to extract the characteristics of local long and short pathways, respectively. Unlike the IDN model [13], three paths are constructed in each part, and different convolution kernels are used for different paths. This allows the model to detect long and short path features at various scales in an adaptive manner. Specifically, it is assumed that the inputs and outputs of the first part are M_{d-1} and O_{PI}. Thus, there are:

$$O_{P1} = \sigma\left(Y^1_{1\times1}\left(\left[\sigma\left(Y^2_{3\times3}(M_{d-1})\right) + \sigma\left(Y^3_{5\times5}(M_{d-1})\right) + \sigma\left(Y^4_{7\times7}(M_{d-1})\right)\right]\right)\right) \tag{6}$$

Where $Y^1_{1\times1}$, $Y^2_{3\times3}$, $Y^3_{5\times5}$, and $Y^4_{7\times7}$ are the first part of the 1 × 1, 3 × 3, 5 × 5, and 7 × 7 convolution functions, respectively; $[\cdot]$ denotes the connection of feature maps obtained from different convolution kernels; and σ denotes the ReLU function[21]. Then, the 64-dimensional O_{P1} feature maps and the M_{d-1} inputs of the MSID blocks are connected to the channel dimension:

$$R = C(S(O_{P1}, 64), M_{d-1}) \tag{7}$$

Where C and S stand for the join operation and the slice operation. In order to combine the recent multiscale data with the earlier data, the 64-dimensional features are derived from S. This might be viewed as the short path information that was remembered. The second portion then gets the long path information using the remaining 64-dimensional feature map as input:

$$O_{P2} = \sigma\left(Y^5_{1\times1}\left(\left[\sigma\left(Y^6_{3\times3}(O_{P1}, 64)\right) + \sigma\left(Y^7_{5\times5}(O_{P1}, 64)\right) + \sigma\left(Y^8_{7\times7}(O_{P1}, 64)\right)\right]\right)\right) \tag{8}$$

Where $Y^5_{1\times1}$, $Y^6_{3\times3}$, $Y^7_{5\times5}$, and $Y^8_{7\times7}$ are the second part of the 1 × 1, 3 × 3, 5 × 5, and 7 × 7 convolution functions, respectively; Last but not least, the input data, short path data, and long path data are all combined:

$$M_d = R + O_{P2} \tag{9}$$

Where M_d denotes the output of the MSID block.

2.4 NSST coefficients prediction

Straight and curved lines cannot be "optimally" represented in wavelet analysis picture functions [22]. The shear waveform transform is a geometric representation that has several scales and resolutions [23]. To maintain the shear wave transform's superiority and prevent the detrimental effects of up-sampling and down-sampling, NSST uses non-subsampled Laplacian pyramid filters [24]. As a result, the NSST exhibits the properties of multi-scale, multi-direction, and translation invariance.

Multiscale decomposition and multidirectional decomposition are the two components of NSST. A modified shear wave filter realizes the multidirectional decomposition, whereas a non-subsampled Laplacian pyramid filter realizes the multiscale decomposition. The non-subsampled Laplacian pyramid filter divides the low-frequency subbands k times, yielding k + 1 high-frequency subbands and one low-frequency subband, in order to capture the singularity of a picture or signal. In order not to use the subsampling operation, the whole process maps the shear-wave filter from a pseudo-polarized grid system to a two-dimensional convolutional computational implementation in Cartesian coordinate system, i.e., it is directly processed in the transform domain. When comparing the high frequency coefficients of NSST and WT, it is evident that NSST can more accurately represent the texture curvature and details. The medical image SR problem is presented in this paper as a prediction problem of NSST coefficients, enabling the MSID network to further preserve richer structural details.

The majority of earlier SR techniques based on CNNs forecasted high-resolution images in the spatial domain, producing outputs that were too smoothed while losing texture features. The introduction claimed that SR approaches in the transform domain can produce more accurate findings than those in the spatial domain. Subsequently, some scholars[18, 19] proposed predicting HR images in the WT domain. However, WT has limitations in directionality, involving only three directions (horizontal, vertical and diagonal), and is not capable of portraying curves. Therefore, the text adopts the superior performance of NSST with better multi-scale, multi-direction and translation invariant properties for HR image prediction. The MSID network can maintain richer structural information outside of the spatial domain by modeling the medical image SR problem as a prediction of NSST coefficients. It is important to note that NSST is a quick and easy approach to boost performance and may be utilized for various SR networks. The previous literature provided a full description of the NSST implementation process [24].

3 Training Performance

3.1 Estimation Indicator

Both quantitative and qualitative evaluations of the suggested method's

performance are made in the experiments. The network performance as well as the picture quality, such as texture changes, are assessed using three metrics: peak signal to noise ratio (PSNR), structural similarity (SSIM), and root mean square error (RMSE) [25]. The following is the calculating formula:

$$PSNR(x,y) = 10 \times \log_{10}\left(\frac{MAX^2}{\frac{1}{N^2}\sum_{i=1}^{N}\sum_{j=1}^{N}\left(x_{i,j}-y_{i,j}\right)^2}\right) \tag{10}$$

$$SSIM(x,y) = \frac{(2\mu_x\mu_y+C_1)(2\sigma_{xy}+C_2)}{(\mu_x{}^2+\mu_y{}^2+C_1)(\sigma_x{}^2+\sigma_y{}^2+C_2)} \tag{11}$$

$$RMSE(x,y) = \sqrt{\frac{1}{N^2}\sum_{i=1}^{N}\sum_{j=1}^{N}\left(x_{i,j}-y_{i,j}\right)^2} \tag{12}$$

Where MAX denotes the maximum gray value; x denotes the predicted image obtained by network training; y denotes the standard high precision image; μ_x denotes the mean of x; μ_y denotes the mean of y; $\sigma_x{}^2$ denotes the variance of x; $\sigma_y{}^2$ denotes the variance of y; σ_{xy} denotes the covariance of xy; C_1 and C_2 are constants.

In addition, the test results in this paper were evaluated by a senior radiologist with more than 10 years of experience in diagnostic imaging, and the mean opinion score (MOS) was used as a criterion for subjectivity assessment [3, 26].

3.2 Image Dataset

To develop a dataset for medical image SR, medical images of the head, brain, lung, abdomen, and bone were combined. Each bodily part is represented by 250 photos from the dataset's 1000 medical photographs. The bone and abdominal photos were used with permission, whereas the head and lung images were chosen from The Cancer Imaging Archive (TCIA) [27]. The training set was made up of 700 medical photos (175 images for each bodily area), while the test set was made up of just 300 images. The majority of the images were created using MRI (T1-weighted imaging, T2-weighted imaging, diffusion-weighted imaging DWI, and fluid flip recovery attenuation series FLAIR) and CT (low density, high density, and mixed density) modalities. In this experiment, the MRI images of the abdomen with an imaging resolution of 320×290 and the CT images of other parts of the body with an imaging resolution of 512×512 were used.

The experiment uses 1,000 original high-resolution medical photos. To create the low-resolution image dataset, the original high-resolution medical images are downscaled by 8*/4* using the conventional Bicubic (bicubic interpolation). These low-resolution and high-resolution datasets form a training set that is fed into the network for training in order to build SR models and finally obtain SR results.

3.3 Training Process

On the 700-image training dataset given in Section 3.1, data augmentation was done. The modified training images' flipping and rotation were taken into

consideration. The original photos are specifically rotated by 90, 180, and 270° before being flipped horizontally. In this way, for each original image there are 4 additional augmented versions. The NSST-MSID network contains 8 MSID blocks. The training medical images are decomposed by one level of NSST to obtain 1 low-frequency subband with 4 high-frequency subbands, which are then cropped into 48 × 48 overlapping 24-pixel slices for training. The initial learning rate for all layers is set to 10-4, and after 50 cycles, the learning rate is reduced by half. The batch input is set to 64. The model was trained on Tesla k80 GPUs in about 9 hours.

3.4 Comparison with other Advanced Methods

In this study, the effectiveness of the suggested strategy is assessed using data from the brain, lung, abdomen, and bone. All of the models are trained using the identical training sets, and the publicly available codes of the comparable methods are used to ensure a fair comparison, including MSRN [28], IDN [13], SRFBN [29], DWSR [18], DMSN [17], RCAN [10], and the present NSST-MSID network. The PSNR, SSIM and RMSE values (scales: 4 × and 8 ×) used for comparison are shown in Tables 1 to 3. It is evident that NSST-MSID network suggested in this paper produces greater PSNR and SSIM values as well as lower RMSE values as compared to the other approaches when tested on the four datasets. This shows that the proposed technique has better image texture variation quality and network performance. Additionally, the perceived realism of the generated SR images is quantitatively evaluated using MOS. In this study, 100 photographs are randomly chosen for validation assessment from a test batch of 300 images. In this study, there is one HR picture for each image and seven subsequent images that have been processed using the seven SR approaches. On a scale of 1 (poor), 2 (fair), 3 (good), and 4 (very good), radiologists were asked to rate the quality of the images (excessive smoothness, artifacts, poor texture, and low signal-to-noise ratio); the MOS was then determined by computing the mean and standard deviation of each approach. The MOS values of the currently proposed NSST-MSID network obtained the greatest MOS when compared to the MOS values of each method for the header dataset (4 ×).

3.5 Ablation Experiment

The influence of the number of MSID blocks T on the network's performance shows that increasing T improves performance, suggesting that a deeper network is preferable. Considering the compromise between accuracy and speed, T=8 is used to construct the NSST-MSID network in the experiments. Incorporating the distillation feature improves the PSNR values for all four sites at a scale of 8× and a number of MSID blocks T = 8. After incorporating the multiscale feature, the PSNR values of all four sites are improved at a scale of 8 × and the number of MSID blocks T = 8. Additionally, since the absolute receptive field of the convolution on various patches is constant, the size of the picture patch has little

to no impact on the network's ability to extract features.

The NSST-MSID network suggested in this paper exhibits a considerable improvement, with NSST predictions outperforming the spatial domain and the other two transform domains. In addition to this, this paper further evaluates the effect of NSST decomposition hierarchy on network performance. Since the more high-frequency layers of decomposition and the more directions, the overhead of the network will increase, so this paper only discusses the high-frequency layers of decomposition with less than 5 layers. Considering the network overhead, this paper selects the results of NSST decomposition of 3 layers. Table 8 shows the PSNR values corresponding to different high-frequency layers decomposed by NSST. As the number of decomposition layers and decomposition directions increase, the learned details are richer and the PSNR values also increase.

4 Conclusion

The NSST-MSID network, a unique super-resolution reconstruction technique for medical images that is based on the NSST domain's MSID network, is presented in this research. By leveraging the NSST to handle the super-resolution reconstruction problem in medical pictures, the suggested method seeks to address the difficulty in getting high-resolution images in medical imaging. Multiple cascaded MSID blocks make up the NSST-MSID network, which is intended to extract multi-scale features from the images and convert low-resolution images into high-resolution ones. This approach formulates the super-resolution task for medical images as the prediction of NSST coefficients, in contrast to earlier approaches that predicted high-resolution images in the spatial domain. Compared to spatial domain techniques, this strategy enables the MSID network to keep rich structural information better. Results from experiments on a collection of medical images show that the NSST-MSID network outperforms competing techniques in terms of PSNR, SSIM, and RMSE. This method achieves better preservation of local texture details and global topological structures in the reconstructed images, resulting in improved medical image reconstruction effect. Overall, this research suggests a unique CNN-based SR network for medical imagery. The network can completely extract the multiscale aspects of medical images since it is made up of a succession of cascaded multiscale information distillation blocks. In order to maintain deeper features than the spatial domain, NSST is added into the network, significantly enhancing SR performance. The results, both quantitative and qualitative, show that the suggested method is superior. A practical answer to the problem of acquiring high-resolution medical images is the NSST-MSID network. By leveraging the NSST domain and the multi-scale information distillation network, this method achieves better preservation of fine details and overall image quality in medical image super-resolution reconstruction. The performance of the NSST-MSID network can be further improved in the future research, and its use in other medical imaging jobs can also be investigated.

References

1. Chaudhari AS, Fang Z, Kogan F, et al. Super-resolution musculoskeletal MRI using deep learning. Magn Reson Med 2018;80:2139-2154.
2. Umehara K, Ota J, Ishida T. Application of Super-Resolution Convolutional Neural Network for Enhancing Image Resolution in Chest CT. J Digit Imaging 2018;31:441-450.
3. Zhu J, Yang G, Lio P, editors. How Can We Make Gan Perform Better in Single Medical Image Super-Resolution? A Lesion Focused Multi-Scale Approach. 2019 IEEE 16th International Symposium on Biomedical Imaging (ISBI 2019); 2019 8-1.
4. Cheng B, Xiao R, Wang J, et al. High Frequency Residual Learning for Multi-Scale Image Classification. 2019.
5. Gupta AK, Seal A, Prasad M, et al. Salient Object Detection Techniques in Computer Vision-A Survey. Entropy (Basel) 2020;22.
6. Rui G, Xiao-Ping S, Dian-Kun JJJoEoHU. Learning a deep convolutional network for image super-resolution reconstruction. 2018.
7. Kim J, Lee JK, Lee KMJI. Accurate Image Super-Resolution Using Very Deep Convolutional Networks. 2016.
8. Tai Y, Yang J, Liu X, editors. Image Super-Resolution via Deep Recursive Residual Network. 2017 IEEE Conference on Computer Vision and Pattern Recognition (CVPR); 2017 21-26.
9. Tai Y, Yang J, Liu X, et al., editors. MemNet: A Persistent Memory Network for Image Restoration. 2017 IEEE International Conference on Computer Vision (ICCV); 2017 22-29.
10. Zhang YaL, Kunpeng and Li, Kai and Wang, Lichen and Zhong, Bineng and Fu, Yun. Image Super-Resolution Using Very Deep Residual Channel Attention Networks. Proceedings of the European Conference on Computer Vision (ECCV) 2018.
11. Tong T, Li G, Liu X, et al., editors. Image Super-Resolution Using Dense Skip Connections. 2017 IEEE International Conference on Computer Vision (ICCV); 2017 22-29.
12. Xu J, Chae Y, Stenger B, et al., editors. Dense Bynet: Residual Dense Network for Image Super Resolution. 2018 25th IEEE International Conference on Image Processing (ICIP); 2018 7-10.
13. Hui Z, Wang X, Gao X, editors. Fast and Accurate Single Image Super-Resolution via Information Distillation Network. 2018 IEEE/CVF Conference on Computer Vision and Pattern Recognition; 2018 18-23.
14. Huang S, Wang J, Yang Y, editors. Image Super-Resolution Reconstruction Based on Multi-scale Residual Learning. 2021 International Conference on Information Technology and Biomedical Engineering (ICITBE); 2021 24-26.
15. Zhou H, Ma Y, Ma Y, et al., editors. Split-based Feedback Network for Image Super-Resolution. 2022 International Conference on Culture-Oriented Science and Technology (CoST); 2022 18-21.
16. Gao SH, Cheng MM, Zhao K, et al. Res2Net: A New Multi-Scale Backbone Architecture. IEEE Transactions on Pattern Analysis and Machine Intelligence 2021;43:652-662.
17. Wang C, Wang S, Ma B, et al., editors. Transform Domain Based Medical Image Super-resolution via Deep Multi-scale Network. ICASSP 2019 - 2019 IEEE International Conference on Acoustics, Speech and Signal Processing (ICASSP); 2019 12-17.
18. Guo T, Mousavi HS, Vu TH, et al., editors. Deep Wavelet Prediction for Image Super-Resolution. 2017 IEEE Conference on Computer Vision and Pattern Recognition Workshops (CVPRW); 2017 21-26.
19. Huang H, He R, Sun Z, et al., editors. Wavelet-SRNet: A Wavelet-Based CNN for Multi-

scale Face Super Resolution. 2017 IEEE International Conference on Computer Vision (ICCV); 2017 22-29.
20. Lim B, Son S, Kim H, et al., editors. Enhanced Deep Residual Networks for Single Image Super-Resolution. 2017 IEEE Conference on Computer Vision and Pattern Recognition Workshops (CVPRW); 2017 21-26.
21. Glorot X, Bordes A, Bengio YJJoMLR. Deep Sparse Rectifier Neural Networks. 2011;15:315-323.
22. Mallat SGJCMP. A Wavelet Tour of Signal Processing: The Sparse Way. 2009.
23. Lim WQ. The Discrete Shearlet Transform: A New Directional Transform and Compactly Supported Shearlet Frames. IEEE Transactions on Image Processing 2010;19:1166-1180.
24. Hou, observations BJIjostiae, sensing r. SAR Image Despeckling Based on Nonsubsampled Shearlet Transform. 2012.
25. Wang Z. Image Quality Assessment : From Error Visibility to Structural Similarity 2004.
26. Seitzer M, Yang G, Schlemper J, et al. Adversarial and Perceptual Refinement for Compressed Sensing MRI Reconstruction. 2018.
27. Clark K, Vendt B, Smith K, et al. The Cancer Imaging Archive (TCIA): maintaining and operating a public information repository. J Digit Imaging 2013;26:1045-1057.
28. Feng XL, Jianxiong %J Applied Intelligence: The International Journal of Artificial Intelligence, Neural Networks,, Technologies CP-S. Multi-scale fractal residual network for image super-resolution. 2021;51.
29. Li Z, Yang J, Liu Z, et al., editors. Feedback Network for Image Super-Resolution. 2019 IEEE/CVF Conference on Computer Vision and Pattern Recognition (CVPR).